Soils and Rocks
An International Journal of Geotechnical and Geoenvironmental Engineering
www.soilsandrocks.com
ISSN 1980-9743
ISSN-e 2675-5475

Influence of the filling process on the behaviour of geotextile tubes

Michael Andrey Vargas Barrantes[1#], Luís Fernando Martins Ribeiro[1], Ennio Marques Palmeira[1]

Article

Keywords
Geotextile tube
Dewatering
Nonwoven geotextile

Abstract

Geotextile tubes can be used to dewater materials such as sludge, sediments or residues aiming at reducing their moisture contents to acceptable levels. The tube filling process can be carried out using one or several filling stages, and the number of stages can influence the tube behaviour in terms of dewatering rate, final shape and geotextile strains, for instance. In this research, laboratory tests were carried out on nonwoven geotextile tubes for the dewatering of a fine-grained material using different numbers of filling stages. The behaviour of the tube was monitored by instrumentation to assess tube geometry, pore pressures, total stresses at the tube base, geotextile strains and retention capacity. Evaluations of the accuracy of some available methods for the prediction of tube behaviour were also made. The results obtained showed that the increase in the number of filling stages resulted in larger final tube height, volume, geotextile strains as well as larger diameters of the soil particles that piped through the geotextile. Predictions of tube behaviour by available methods showed varying degrees of accuracy depending on the tube parameter considered.

1. Introduction

Geosynthetics have been used for various functions in geotechnical and environmental engineering projects, such as soil reinforcement, drainage, filtration and as barriers, for instance. Among the reasons why geosynthetic have gained considerable acceptance over the years are: easy transportation to working sites, quick installation, repeatable properties and savings in the use of natural construction materials. These characteristics can yield to significant cost savings compared to traditional geotechnical alternatives and provide environmentally friendly engineering solutions.

The increase in industrial activities causes large amounts of waste to be generated with large percentages of fines, varying contents of liquid and, not seldom, contaminant substances. This creates difficulties for the disposal of these materials, and alternative management techniques must be necessary (Moo-Young et al., 2002; Muthukumaran & Ilamparuthi. 2006; Bourgès-Gastaud et al., 2014). The technique of using geotextile tubes has been considered an efficient and economical solution for moisture content reduction and safer disposal of wastes (Maurer et al., 2012). To better understand the dewatering behaviour of geotextile tubes, several laboratory studies have been carried out over the last decades (Moo-Young et al., 2002; Moo-Young & Tucker, 2002; Koerner & Koerner, 2006; Muthukumaran & Ilamparuthi, 2006; Lawson, 2008; Liao & Bathia, 2008; Satyamurthy & Bhatia, 2009; Cantré & Saathoff, 2011).

Several works in the literature have reported the use of geotextile tubes for a series of purposes such as drying sludge or sewage material in wastewater treatment plants, rehabilitation of slopes, protection of coastal areas by means of breakwaters, slope buttresses and protection dikes, among others (Leshchinsky et al.,1996; Plaut & Suherman, 1998; Koh et al., 2020, Pilarczyk, 2000; Koerner & Koerner, 2006; Lawson, 2008; Yan and Chu, 2010; Yee et al., 2012; Yee & Lawson, 2012).

A specific problem faced in the field of engineering is how to efficiently dispose sludge with high water-content such as dredged sediment, industrial waste, wastewater treatment sludge, and mining tailings (Bourgès-Gastaud et al., 2014). In addition, the use of geotextile tubes for the dewatering of tailings in mining plants has increased in acceptance because of drainage efficiency and lower investments and maintenance costs (Assinder et al., 2016; Newman et al., 2004; Li et al., 2016; Wilke et al., 2015). Results presented by Yang et al, (2019) show that the application of geotextile tubes in tailings storage structures represent a good alternative for fine tailings disposal.

The typical process of dewatering with geotextile tubes consists of several stages of filling and dewatering (Yee & Lawson, 2012). During the filling stage, the sludge material

#Corresponding author. E-mail address: ma12vargas@gmail.com.
[1]Universidade de Brasília, Departamento de Engenharia Civil e Ambiental, Brasília, DF, Brasil.

Submitted on October 11, 2022; Final Acceptance on March 19, 2023; Discussion open until November 30, 2023.

https://doi.org/10.28927/SR.2023.010522

is pumped into the tube under turbulent conditions followed by the outflow of the liquid, with sedimentation of particles in the lower part of the tube. The filling and dewatering stages are then repeated up to the maximum operational capacity of the system. Despite the success in use of geotextile tubes, some uncertainties remain regarding important design and construction issues.

Some studies (Lawson, 2008; Yee & Lawson, 2012, Wilke & Cantré, 2016, Ratnayesuraj & Bhatia 2018, Kim & Dinoy, 2021) admit tube filling and dewatering processes in a single or multiple stages. The number of stages can influence pore pressure generation (Zhang et al., 2022), strains and tensile forces in the geotextile (Plaut & Filz, 2008, Kim et al., 2020) as well as limiting the accuracy of predictions of tube behaviour from theoretical solutions.

This paper presents and discusses results of large-scale laboratory tests to investigate the influence of varying numbers of filling stages on geotextile tube behaviour considering the development of pore pressures and total stresses in the filling material, as well as the strains in the geotextile. For this purpose, tubes were filled with slurry in a single stage and in three stages. The results obtained in the experiments are presented and discussed in the following items.

2. Experimental

2.1 Materials

The infill material used in the experimental program consisted of a mixture of a lateritic silty clay and water in the form of a slurry with a concentration (in mass) of solids of 50%. The grain size analysis of the soil carried out using a laser beam grain size analyzer (Microtrac) revealed values of D_{85} (diameter for which 85% of the remaining particle diameters are smaller than that value, Table 1) of 0.063 mm and 0.259 mm in tests with and without dispersing agent, respectively, D_{50} of 0.027 mm and 0.120 mm, D_{10} of 0.0036 mm and 0.040 mm, liquid limit of 37% and plastic limit of 28%. The predominant soil mineral is gibbsite, an in its natural state the soil fabric presents macropores and many aggregates (Burgos, 2016). Table 1 presents the main geotechnical properties of the soil used in the test.

A nonwoven, needle-punched, geotextile made of polyester continuous filaments was used. The mass per unit area of the geotextile is equal to 200 g/m^2 and its filtration opening size is equal to 0.115 mm. The geotextile tubes had a length of 1 m and a diameter of 0.8 m. The main geotextile properties are summarized in Table 2.

Table 1. Soil Properties.

Proprieties	Values
D_{10} (mm)(1)	0.040/0.0036(2)
D_{50} (mm)	0.120/0.027
D_{85} (mm)	0.259/0.063
Coefficient of uniformity	3.7/8.4
% smaller than 0.075 mm	29/87
Liquid Limit (%)*	37
Plastic Limit (%)*	28
Plasticity Index (%)*	9
SUCS Classification	CL
AASHTO Classification	A-4
MCT Classification	LA-LA'

(1) D_n = diameter of the particle for which n% of the remaining particles are smaller. (2) Values on the left are from tests without the use of dispersing agent and values on the right with the use of dispersing agent.

***Source:** Burgos (2016).

Table 2. Geosynthetics properties.

Propriety	Values
Polymer (1)	PET
M_A (g/m^2)	200*
t_{GT} (mm)	2.2*
O_{95} (mm)(2)	0.115
J_5 (kN/m)(3,6)	11.5
'T_{max} (kN/m)(4,6)	9.8
ε_{max} (%)(5,6)	83-100

(1) PET= polyester; M_A = mass per unit area (ASTM D5261); t_{GT} = nominal thickness (ASTM D 5261). (2) O_{95} = filtration opening size (ASTM D6767). (3) J5 = secant tensile stiffness at 5% strain. (4) *Tmax* = tensile strength. (5) εmax = maximum tensile strain. (6) Wide-strip tensile tests as per ASTM D4595. * Data provided by the manufacturer.

2.2 Equipment

A channel (6 m long x 1.5 m high; 1 m wide) was used in the experiments. A section at one of the extremities of the channel was used for the mixing of the soil with water. The rest of the channel length was used to construct the geotextile tubes (Figure 1). The sides of the channel are transparent to allow the view of the deformed shape of the tube during the test. Two layers of lubricated plastic were applied to the channel walls to minimize friction between the geotextile and the glass. Soil was continuously and uniformly mixed with water to form a slurry with a unit weight of 13.5 kN/m^3 using of a 3000 watts power pump prior to the inflow of the slurry in the tube. The geotextile tubes were cylindrical, with a diameter of 0.8 m and a length of 1 m. The geotextile tube rested on a rigid platform at the bottom of the channel.

The tube was instrumented with electric total stress cells and pore pressure transducers installed at its base, as shown in Figure 2. A standpipe connected to the tube base was also installed. The deformation of the tube was measured at several points along its perimeter by monitoring the deformed shape of a square meshes (20 mm wide) printed along the surface of the tube in its central region (Figure 2).

The tests started with the preparation of the soil slurry with a concentration (in mass) of solids of approximately

Figure 1. View and dimensions of the equipment (a) View of the mixing and test sections; (b) Dimensions of the channel.

50%. The process of mixing and filling was carried out by means of a dredge pump. The injection flow rate of the mixture inside the geotextile tubes was equal to 0.75 l/s. The tubes were filled with a single filling step or with three filling steps. The filling stage lasted until the tubes reached an initial height of 450 mm.

After the end of the tests, the soil particles that piped through the geotextile were collected for grain size analysis. A laser beam particle analyzer (Microtrac) was used for the measurement of the diameters of the piped particles.

3. Results

3.1 Volume reduction and change in dewatering rate

Figure 3 shows the volume of water drained from the tubes over 4 weeks for the two tests performed, which are identified by the codes GT-1FS (single filling stage) and GT-3FS (three filling stages). Stabilization of the readings at the end of the second, third and fourth week in the test GT-3FS can be noted. For the case of the GT-1FS test, the same stabilization of drained water volume can be observed after 13 days after filling. The use of three filling stages led

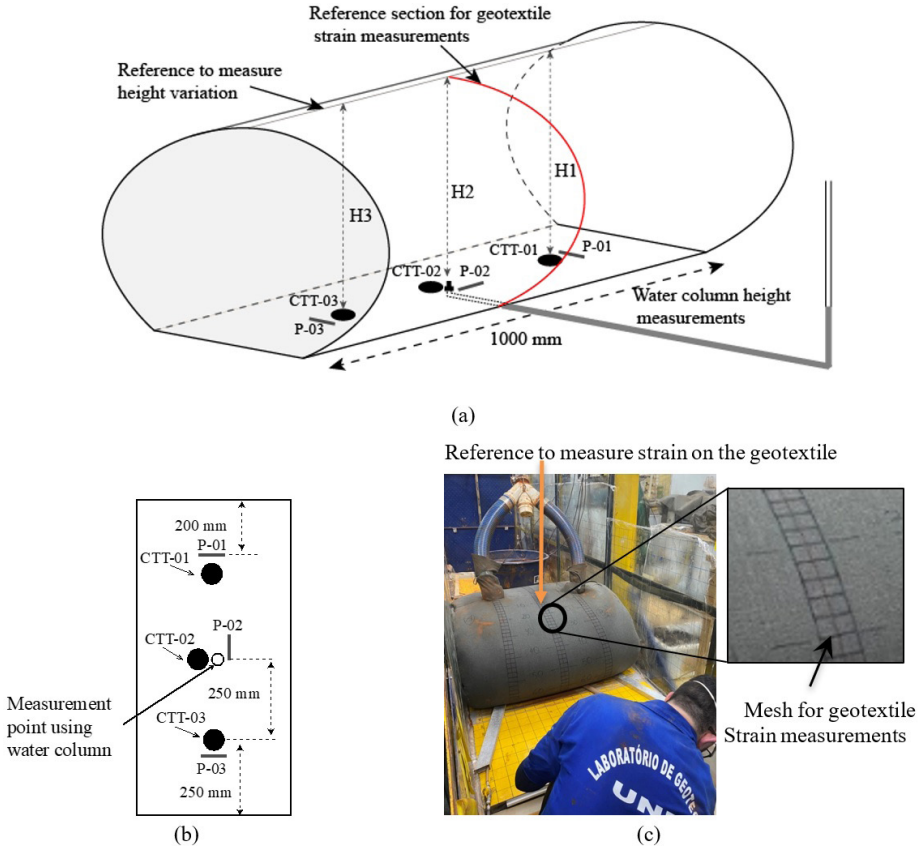

Figure 2. Instrumentation of the tube (a) Location of pressure cells and pore pressure transducers; (b) Location of the instruments at the base of the geotextile tube; (c) Square mesh printed along the surface of the tube for geotextile strain measurements.

to a volume of drained water 29% higher compared to the test with a single filling stage.

The tube height variation with time was recorded throughout the test and is depicted in Figure 4. It can be noted that the magnitude of the tube height increases at the beginning of each filling stage decreased in test GT-3FS. According to Yee & Lawson (2012), as the number of draining stages increases, the volume of solids and flakes deposited in the tube also increases, thus decreasing the variation in height between each filling stage. A similar behaviour of the two tests can be observed in the first two weeks, with just a slight difference in height at the end of the second week when compared with test GT-3FS. The formation of layers of sedimented material at the bottom of the tube occurs more quickly after the filling process, associated with a greater output of free water (Figure 3). A transition from a process dominated by dewatering to another dominated by consolidation takes place, as described by Lawson (2008).

The volume of slurry injected in the tube was measured for each filling stage. Figure 5 presents the variation of the tube total volume with time during tests GT-1FS and GT-3FS. The change in contained slurry volume within the geotextile tube and the change in concentration of solids are interrelated (Lawson, 2008). For a single filling-dewatering cycle, the expected increase in solids concentration can be determined for a given reduction in contained slurry volume from (Lawson, 2008):

$$S_t = \frac{\left(\frac{1}{1-\Delta V_t}\right)\left(\frac{S_0}{1-S_o}\right)}{1+\left(\frac{1}{1-\Delta V_t}\right)\left(\frac{S_o}{1-S_o}\right)} \quad (1)$$

Where St is the concentration of solids at time t, ΔV_t is the contained slurry volume reduction over time t and S_0 is the initial concentration of solids.

From the variation of the slurry volume recorded in the test GT-1FS in Figure 5a, it is possible to obtain the variation of the theorical concentration with time using Equation 1, as shown in Figure 5b. There is a gradual reduction in volume as the water drains, consequently leading to an increase in concentration of solids with time. Higher rates of concentration increase were observed in the first 5 days of testing.

According to Yee & Lawson (2012), once the retained volume inside the tube and the solids concentration stabilize, the process starts to be dominated mainly by consolidation, when small changes of volume of drained water, height of the geotextile tube and dewatering rate (Figure 3, 4, 5 and 6, respectively) take place at a much smaller rate.

The recorded volume of effluent from the geotextile tube over time was used to calculate the variation of dewatering rate with time, as shown in Figure 6. The peaks at 14 and 24 days correspond to the start of the 2nd and 3rd filling stages in test GT-3FS test. It can be noticed that in this test, after the first filling stage, the dewatering rate dropped to nearly zero after 13 days, but this time was smaller in the following steps, showing the drainage capacity of the enveloping geotextile was not compromised during the test duration. For test GT-1FS almost zero drainage was observed after approximately 15 days of testing.

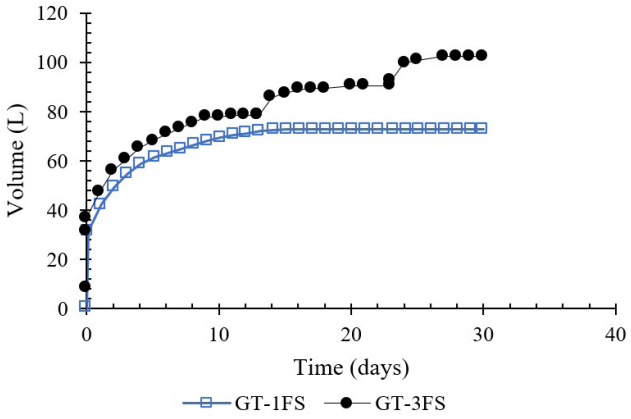

Figure 3. Accumulated volume of water drained during the tests.

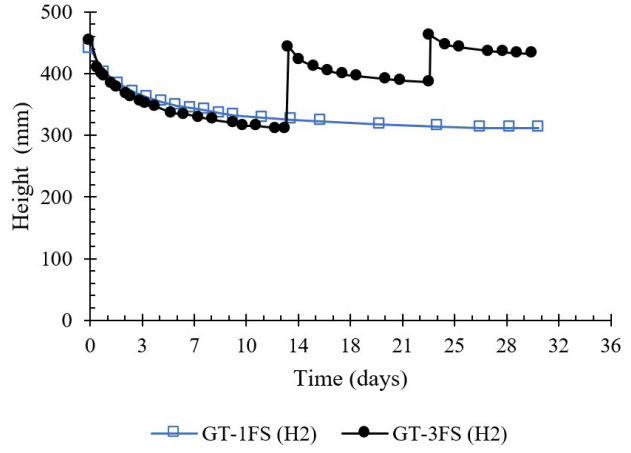

Figure 4. Variation of tube height with time.

3.2 Pore pressures and total stresses

Figure 7 presents the variation of pore pressure at the base of the tube with time. As expected, maximum pore pressures occur at the start of the filling stage in test GT-1FS and GT-3FS. After filling, the pore pressure transducers (P-01, P-02 and P-03, Figure 2) recorded maximum pore pressure values of 3.45 kPa, 2.52 kPa and 3.12 kPa in test GT-1FS (Figure 7a). Afterwards, a continuous reduction of pore pressure with time can be observed. After 4 weeks of testing, the pore pressures varied between 0 to 0.5 kPa, depending on the pore pressure transducer considered.

Maximum values of a 5.5 kPa, 5.28 kPa and 5.98 kPa in test GT-3FS (Figure 7b) were recorded by the pressure

transducers P-01, P-02 and P-03 (Figure 2). During each dewatering stage, the pore pressures gradually decreased. After 4 weeks of testing, the pore pressures varied between 0.26 kPa to 0.46 kPa. Initial larger values of pore pressures recorded after tube filling in test GT-3FS in comparison to those in test GT-1FS are likely to be a consequence of the impact of the jet of the inflow slurry on the pressure transducers at the tube base at the early stages of testing. The direction of this inflow slurry jet could not be efficiently controlled at those testing stages.

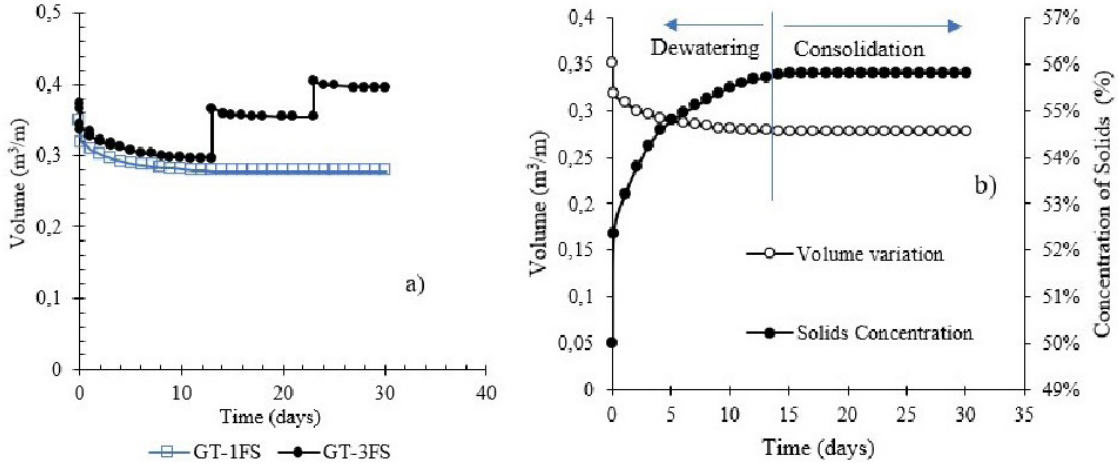

Figure 5. Variation of tube volume and solids concentration with time (a) Volume variation versus time; b) Volume and concentration of solids versus time - GT-1FS.

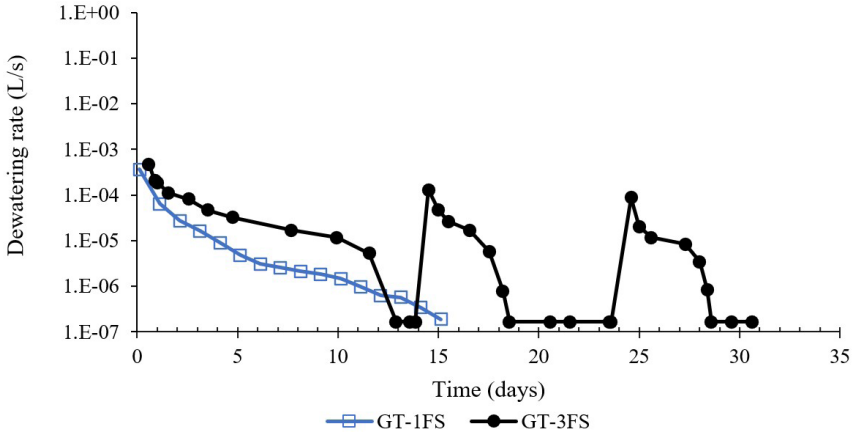

Figure 6. Dewatering rate variation with time.

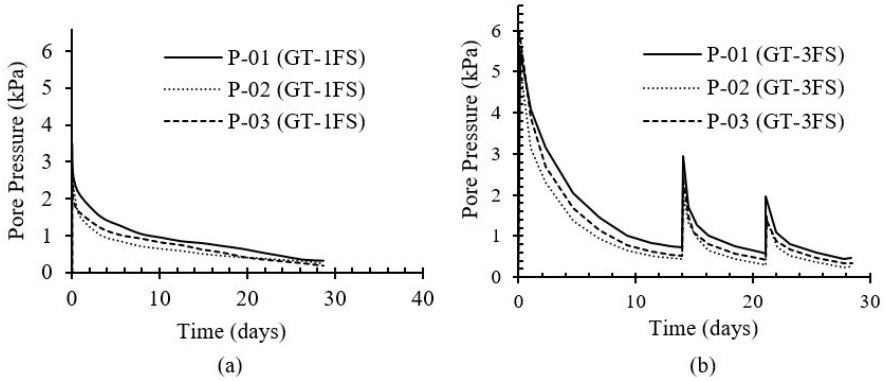

Figure 7. Pore pressure variation with time; a) GT-1FS; b) GT-3SF test.

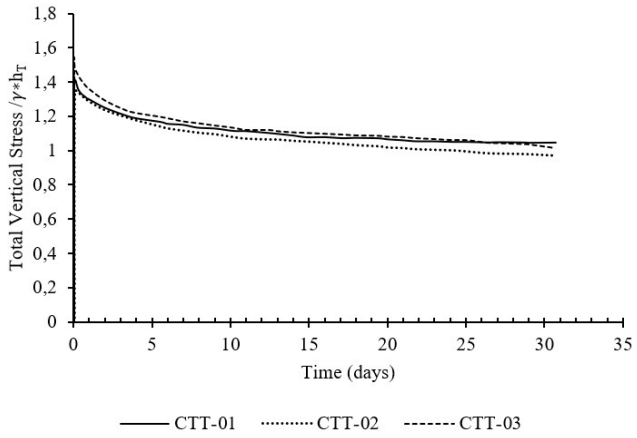

Figure 8. Normalized total pressure at the tube base versus time - test GT-1FS test.

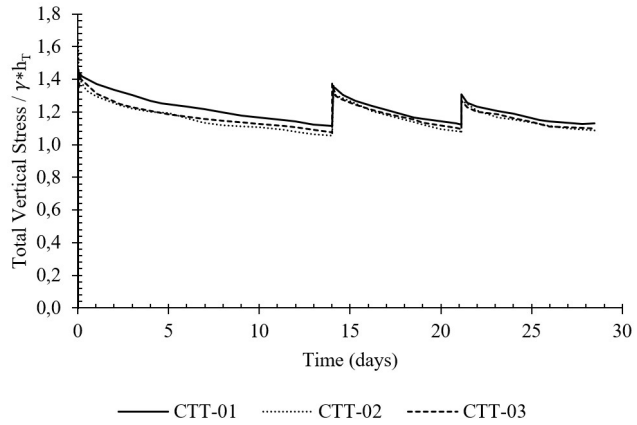

Figure 9. Normalized total pressure at the tube base versus time - GT-3FS.

Figure 8 shows the variation of normalized vertical stress at the tube base with time obtained in test GT-1FS. The total vertical stress at the base was normalized by the product $\gamma.h_T$, where γ is the final unit weight of the soil and h_T is the final tube height. Higher initial vertical stresses are a consequence of the filling process, caused by the impact of the slurry jet on the stress cells. A decrease in normalized total vertical stress due to dewatering can be noted throughout the test until values between 1.05 and 0.97 are reached.

The variation of normalized total vertical stresses at the base of the tube for test GT-3FS is depicted in Figure 9. Similar initial vertical stresses as those observed in test GT-1FS can be noted, followed by reductions with time. In comparison to test GT-1FS, a slight increase in the final vertical stress with the increase in the number of filling stages can be observed due to the slightly greater final soil density at the end of test GT-3FS. In this case, the normalized total vertical stress varied between 1.09 to 1.13 at the end of the last dewatering stage.

3.3 Geotextile strains

Figure 10 shows the variation of geotextile strain along the tube perimeter at the end of tests GT-1FS and GT-3FS, after dewatering stages. The maximum tensile strain was reached at the crown of the tube in both tests decreasing towards the tube base. The strains measured in test GT-3FS were larger than in test GT-1FS along the entire tube perimeter, showing the effect of multiple filling stages on geotextile strain mobilization. As the volume of filling material increased in the tube, so does the geotextile strains.

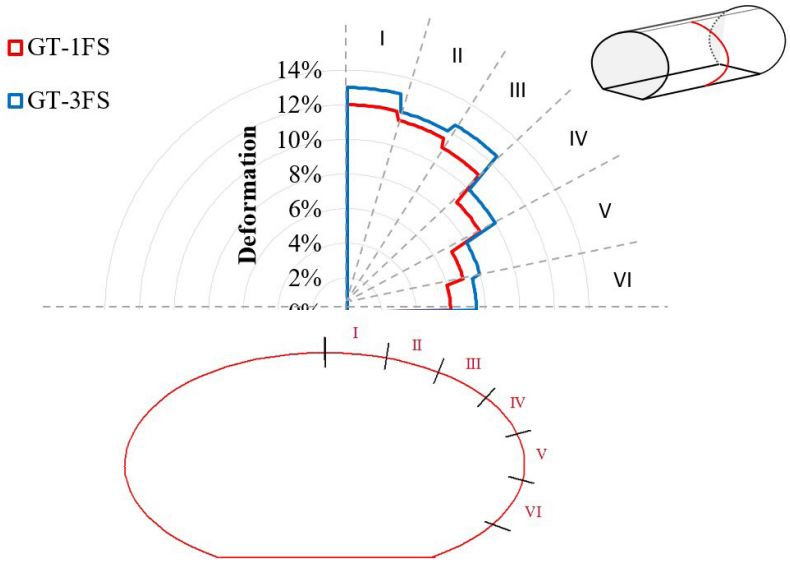

Figure 10. Variation of tensile strain along tube perimeter in tests GT-1FS and GT-3FS.

3.4 Dimensions of the particles that piped through the geotextile.

Figure 11 shows the grain size distribution of the particles (tests without dispersing agent) that piped through the geotextile during the tests, as well as the gradation curve for the particles of the original soil for comparison. This figure shows that the maximum value of the diameter of the particles that piped through the geotextile (taken as d_{95}, which is the particle diameter for which 95% of the remaining particles are smaller) was equal to 0.073 mm in test GT-1FS and 0.093 mm in test GT-3FS, which are values smaller than the filtration opening size of the geotextile (O_{95} = 0.115 mm, Table 2). Thus, the increase in the number of filling stages seems to have caused the piping of coarser material through the geotextile.

It should be pointed out the no flocculating agent was added to the slurry in the current tests and that the geotextile layer is tensioned in this type of application. However, Palmeira et al. (2019) and Palmeira (2020) reported little variation in filtration opening sizes of geotextiles submitted to tension under plane strain conditions.

The total mass of the soil piped through the geotextile was very small, but greater in the case of test GT-3FS (8.51 g against 6.06 g in test GT-1FS). Therefore, despite the small values of piped mass, increasing the number of filling stages resulted in 40.4% increase in piped soil mass. In terms of the total superficial area of the geotextile tube available for particles piping, the values obtained were 3.39 g/m^2 for test GT-3FS and 2.41 g/m^2 for test GT-1FS.

4. Comparisons between predictions and measurements

Predictions of tube volume, tube geometry and geotextile strains were compared to the values measured in the tests. Because the theoretical methods investigated consider a single filling stage in their formulations, emphasis will be given to the comparisons between theoretical predictions and measurements taken in test GT-1FS. In addition, the methods require the knowledge of the pressure (p) employed to fill the tube for the predictions of tube deformations and geotextile tensile forces. In the present study, the average maximum pore pressure measured (3.01 kPa) by the pore pressure transducers during tube filling was adopted in the calculations, since the filling pressure varies during the filling process and the maximum pore pressure value measured would represent more critical filling conditions to the mobilization of strains in the tube.

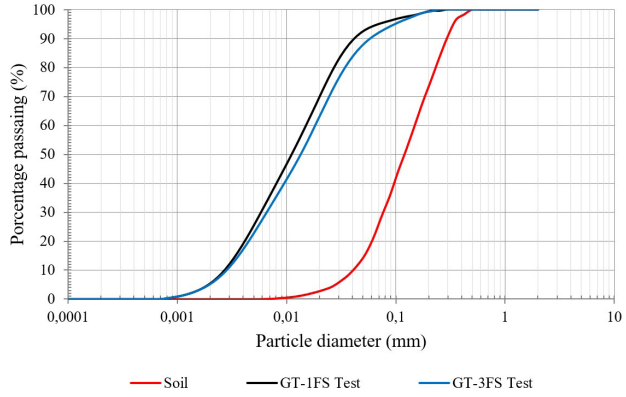

Figure 11. Gradations of the soil particles that piped through the geotextile.

4.1 Tube volume

An empirical relationship which estimates the volume of a geotextile tube as a function of its length, filling height and theoretical diameter was proposed by Yee et al. (2012). According to the authors, satisfactory predictions can be obtained for filling height ratios $h_T/D_T < 0.7$ by the following equation:

$$V_T = L_T D_T^2 \left[\left(\frac{h_T}{D_T} \right)^{0.815} - \left(\frac{h_T}{D_T} \right)^{8.6} \right] \quad (2)$$

Where V_T is the volume of the geotextile tube, L_T is the length of the geotextile tube, h_T is the height of the tube and D_T is the theoretical tube diameter.

The comparison between predicted and measured volume variation with time for test GT-1FS is shown in Figure 12a. Deviations between predicted and measured values can be observed. Equation 2 overpredicted the tube volume by approximately 18% throughout the test. The variation of the geotextile tube volume for test GT-3FS is shown in Figure 12b. In this case, a better agreement between predicted and measured values can be noted, particularly during the last dewatering stage. Up to the 3rd dewatering stage, in average, Equation 2 overpredicted the tube volume by approximately 10% (Figure 12b), but the accuracy of the prediction improved at the end of each dewatering stage.

4.2 Tube geometrical characteristics

The accuracy of available solutions (Guo et al., 2014; Plaut & Suherman, 1998; Lawson, 2008) for the estimate the final shape and dimensions of the tube and the average vertical stress at base were also investigated. Figure 13 shows the comparison between the final cross-section of the tube at the end of the filling stage in test GT-1FS and the prediction by Plaut & Suherman (1998). The method provided an accurate prediction for the tube height (4.5% deviation) and maximum width (5.5% deviation), but underpredicted its tube base width by 20%.

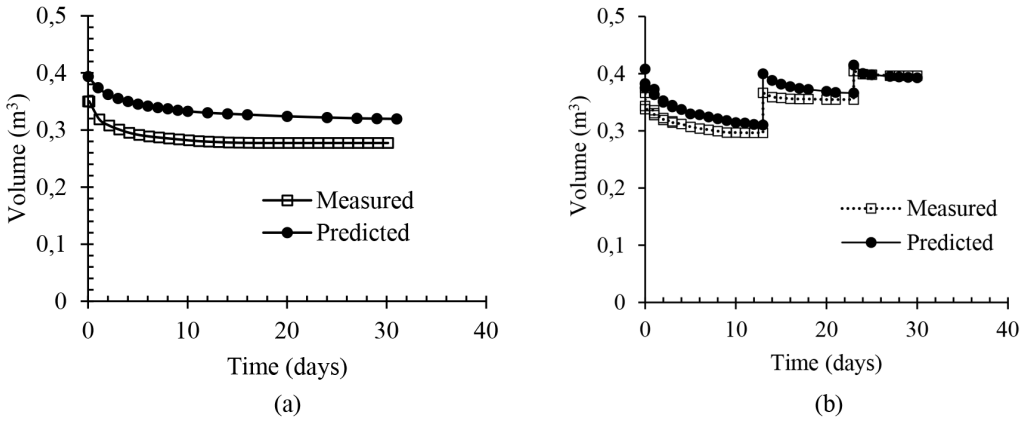

Figure 12. Comparison between predicted and measured volume retained on the geotextile tube (a) Volume variation in test GT-1FS; (b) Volume variation in test GT-3FS.

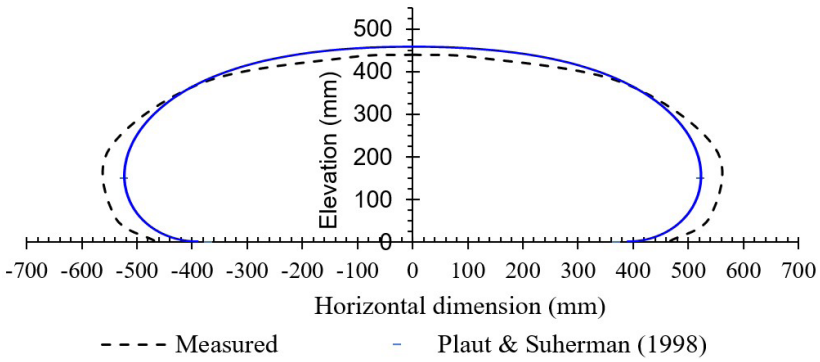

Figure 13. Predicted and measured tube cross-section in test GT-1FS at the end of the filling stage.

Figure 14 presents comparisons between predicted and measured tube height and base width at the end of the filling stage of test GT-1FS. The predictions deviated from the measured values between 4.5% and 29.5%, with the best accuracy being obtained by the predictions by Lawson (2008) and Plaut & Suherman (1998). Guo et al. (2014) over predicted the tube height by 29.5%. All three methods investigated underpredicted the tube base width, with deviations of 13.5% (Lawson), 20.0% (Plaut and Suherman) and 37.3% (Guo et al.).

Comparisons between predicted and measured tube cross-section area, maximum width and the total vertical stress at the base of the tube are depicted in Figure 15. In this figure the vertical stress is normalized by the product of the soil slurry unit weight (13.5 kN/m^3) and the final tube height at the end of the filling stage. The predictions of tube cross-section area deviated from the measurements by 4.7%, 11.6% and 9.3%, for the methods of Guo et al. (2014), Lawson (2008) and Plaut & Suherman (1998), respectively. Regarding predictions of maximum width by Guo et al. (2014), Lawson (2008) and Plaut & Suherman (1998), the deviations from the measured values were 14.5%, 9.1% e 5.5%, respectively.

The predicted values of normalized total vertical stress at the base of the tube compared well with the measurements (Figure 15), with deviations of 2.1% for Lawson (2008) and 2.6% for Plaut & Suherman (1998) methods, respectively.

4.3 Geotextile forces

Table 3 shows maximum and minimum mobilized tensile forces in the tube in tests GT-1FS and GT-3FS. The tensile forces were calculated as the product between the measured tensile strains and the geotextile tensile stiffness (11.5 kN/m, Table 2). Table 3 also presents the predictions of tensile forces by Plaut & Suherman (1998) and Guo et al. (2014) (single filling stage assumed). The mobilized tensile forces in test GT-1FS varied between 0.81 kN/m and 1.49 kN/m after filling (Table 3) depending on the location along the tube perimeter considered. Plaut & Suherman's method predicted a value of 1.26 kN/m for the geotextile tensile force. Thus, the tensile force predicted by that method was closer to the maximum geotextile tensile force measured, but with a deviation of 15.4%. On the other hand, Guo et al. (2014) predicted a tensile force of 1.96 kN/m, which is 31.5% greater than the maximum value measured during the test.

Table 3. Mobilized and predicted geotextile tensile forces at the end of the filling stage and at the end of the test.

Phase	Range	GT-1FS (kN/m)	GT-3FS (kN/m)	Plaut & Suherman (1998) (kN/m)	Guo et al. (2014) (kN/m)
After filling	Maximum	1.49	1.38	1.26	1.96
	Minimum	0.81	0.81		
End of the test	Maximum	1.38	1.49		
	Minimum	0.69	0.86		

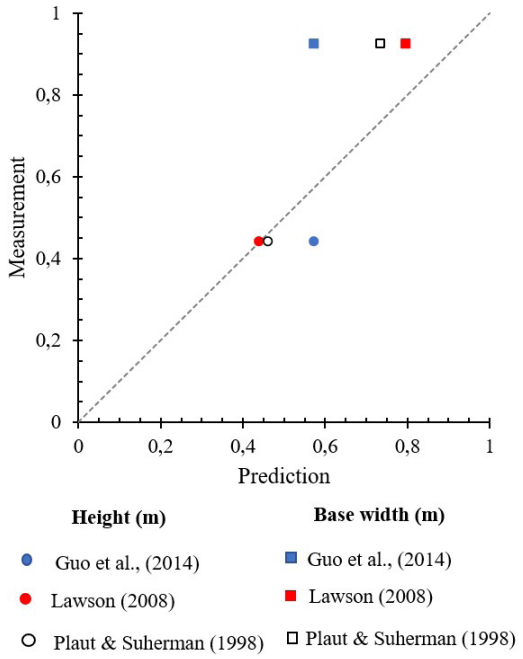

Figure 14. Comparisons between predicted and measured tube dimensions – Test GT-1FS.

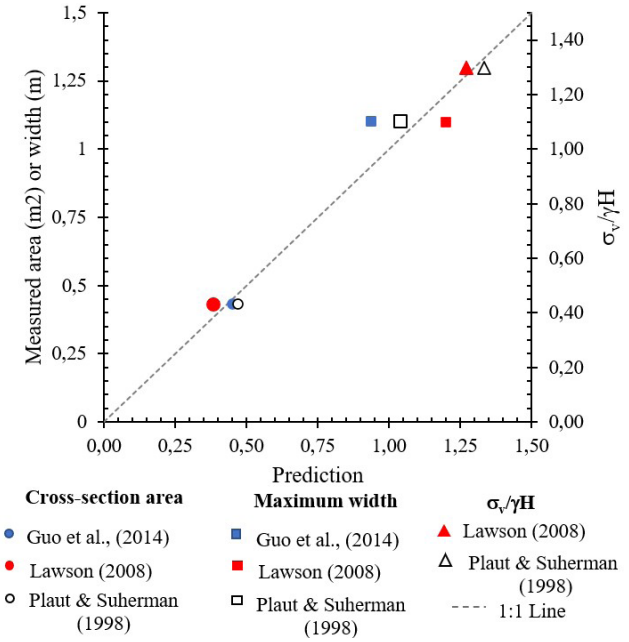

Figure 15. Comparisons between predicted and measured tube dimensions and vertical stresses at the tube base after filling - Test GT-1FS.

5. Conclusions

This work presented an experimental study on the behaviour of geotextile tubes filled with slurry in one and in three filling stages. A large equipment was used to simulate the filling and dewatering stages of the tube and geotechnical instrumentation provided relevant information to understand the tube behaviour. The main conclusions obtained in this study are summarized below.

The use of three filling stages significantly increased the tube final height and volume at the end of the test. Larger geotextile strains were reached in the test with three filling stages, with the maximum strain occurring at the tube crest in both tests. Despite taking much time to fill the tube, the use of multiple filling stages is more efficient regarding final tube height and storage capacity.

The geotextile used was efficient in dewatering the slurry and reducing the pore pressures inside the tube. Particles smaller than the geotextile filtration opening size were capable of piping through the geotextile, but in very small quantities, but larger in size and in quantity in the test with three filling stages.

Regarding comparisons between predictions by methods available in the literature and measurements, deviations ranging from 4.5% to 37.3% between predicted and measured values were observed, depending on the tube parameter and method considered. More accurate predictions were obtained for the tube cross-section area (deviations between 4.7% and 9.3%) and poorer predictions for the tube base width (deviations between 13.5% and 37.3%). Deviations between predicted and measured tube height varied between 4.5% and 29.5%, depending on the method considered. Smaller deviations (2.1% and 2.6%) from the measured values were obtained for the predictions of total vertical stress at the tube base. Deviations of 15.4% and 31.5% were obtained for the predictions of geotextile tensile forces. In general, the relations presented by Lawson (2008) provided the best estimates for the tube behaviour for the conditions of the tests performed.

The results obtained in the study describe herein showed the efficiency of using geotextile tubes for the dewatering of

slurries. However, further research in necessary, particularly for the development of methods to predict the behaviour of geotextile tubes subjected to multiple filling stages.

Acknowledgements

The authors would like to thank the following institutions for their help in the research activities described in this paper: The University of Brasília, CNPq- National Council for Scientific and Technological Development, Capes-Brazilian Ministry Education, Federal District Foundation for Research Support-FAPDF and the geosynthetic manufacturer.

Declaration of interest

The authors have no conflicts of interest to declare. All co-authors have observed and affirmed the contents of the paper and there is no financial interest to report.

Authors' contributions

Michael Andrey Vargas Barrantes: conceptualization, visualization, formal analysis, data gathering, data validation & writing. Ennio Marques Palmeira: conceptualization, methodology, visualization, supervision, formal analysis, writing – review & editing. Luis Fernando Martins Ribeiro: conceptualization, supervision, formal analysis, writing – review & editing.

Data availability

All data produced or examined during the current study are included in this article.

List of symbols

h_T	height of the tube (m)
t	time (s)
t_{GT}	geotextile thickness (m)
ASTM	American Society of Testing Materials
CTT	total stress cell
D_n	diameter of the particle for which n% of the remaining particles are smaller (m)
D_T	theoretical tube diameter (m)
J_5	secant tensile stiffness at 5% strain (N/m)
L_T	length of the tube (m)
M_A	geotextile mass per unit area (g/m2)
O_{95}	filtration opening size (m)
P	pore pressure transducer
PET	polyester
S_o	initial concentration of solids (dimensionless)
S_t	concentration of solids (dimensionless)
T_{max}	geotextile tensile strength (N/m)
V_T	volume of the geotextile tube (m3)
Δ_{Vt}	slurry volume reduction (m3)
ε_{max}	maximum geotextile tensile strain (dimensionless)

References

Assinder, P.J., Breytenbach, M., & Wiemers, J. (2016). Utilizing geotextile tubes to extend the life of a Tailings Storage Facility. In: *Proceeding of the First Southern African Geotechnical Conference*, Sun City, South Africa, 5-6 May. Retrieved in October 11, 2022, from https://www.huesker.es/fileadmin/media/Scientific_Revised_Paper/P761_Utilizing_geotextile_tubes_to_extend_the_life_of_a_Tailings_Storage_Facility_.pdf

Bourgès-Gastaud, S., Stoltz, G., Sidjui, F., & Touze-Foltz, N. (2014). Nonwoven geotextiles to filter clayey sludge: an experimental study. *Geotextiles and Geomembranes*, 42(3), 214-223.

Burgos, L.J.F. (2016). *Influência da microestrutura no comportamento mecânico dos solos tropicais naturais e compactados* [Master's dissertation]. Universidade de Brasília.

Cantré, S., & Saathoff, F. (2011). Design parameters for geosynthetic dewatering tubes derived from pressure filtration tests. *Geosynthetics International*, 18(3), 90-103.

Guo, W., Chu, J., Nie, W., & Yan, S. (2014). A simplified method for design of geosynthetic tubes. *Geotextiles and Geomembranes*, 42, 421-427.

Kim, H.J., & Dinoy, P.R. (2021). Two-dimensional consolidation analysis of geotextile tubes filed with fine-grained material. *Geotextiles and Geomembranes*, 49, 1149-1164.

Kim, H.J., Park, T.W., Dinoy, P.R., & Kim, H.S. (2020). Performance and design of modified geotextile tubes during filling and consolidation. *Geosynthetics International*, 28(2), 125-143. http://dx.doi.org/10.1680/jgein.20.00035.

Koerner, G.R., & Koerner, R.M. (2006). Geotextile tube assessment using a hanging bag test. *Geotextiles and Geomembranes*, 24(2), 129-137.

Koh, J. W., Chew, S. H., Chua, K. E., Yim, H. M. A., & Gng, Z. X. (2020). Effect of construction sequence on the performance of geotextile tubes in a containment bund. *International Journal of GEOMATE*, *74*, 1-7.

Lawson, C.R. (2008). Geotextile containment for hydraulic and environmental engineering. *Geosynthetics International*, 15(6), 384-427.

Leshchinsky, D., Leshchinsky, O., Ling, H.I., & Gilbert, P.A. (1996). Geosynthetic tubes for confining pressurized slurry: some design aspects. *Journal of Geotechnical Engineering*, 122(8), 682-690.

Li, Q.Y., Wang, H.D., Ma, G.W., Li, Z.J., Zhou, H.M., & Cui, X. (2016). An experimental study of the mechanical performance of tailings dam geofabriform. *Yantu Lixue*, 37(4), 957-964. [in Chinese]

Liao, K., & Bathia, S. K. (2008). Geotextile tube dewatering: filtration criteria. In *The First Pan American Geosynthetics*

Conference & Exhibition (pp. 506-513). Cancun, Mexico: IFAI.

Maurer, B.W., Gustafson, A.C., Bhatia, S.K., & Palomino, A.M. (2012). Geotextile dewatering of flocculated, fiber reinforced fly-ash slurry. *Fuel*, 97, 411-417.

Moo-Young, H.K., & Tucker, W.R. (2002). Evaluation of vacuum filtration testing for geotextile tubes. *Geotextiles and Geomembranes*, 20, 191-212.

Moo-Young, H.K., Gaffney, D.A., & Mo, X. (2002). Testing procedures to assess the viability of dewatering with geotextile tubes. *Geotextiles and Geomembranes*, 20(5), 289-303.

Muthukumaran, A.E., & Ilamparuthi, K. (2006). Laboratory studies on geotextile filters as used in geotextile tube dewatering. *Geotextiles and Geomembranes*, 24, 210-219.

Newman, P., Hodgson, M., & Rosselot, E. (2004). The disposal of tailings and mine water sludge using geotextile dewatering techniques. *Minerals Engineering*, 17, 115-121.

Palmeira, E.M. (2020). A review on some factors influencing the behavior of nonwoven geotextile filters. *Soil & Rocks*, 43(3), 351-368. http://dx.doi.org/10.28927/SR.433351.

Palmeira, E.M., Melo, D.L.A., & Moraes-Filho, I. (2019). Geotextile filtration opening size under tension and confinement. *Geotextiles and Geomembranes*, 47, 566-576. http://dx.doi.org/10.1016/j.geotexmem.2019.02.004.

Pilarczyk, K.W. (2000). G*eosynthetics and geosystems in hydraulic and coastal engineering* (913 p.). A.A. Balkema Publisher.

Plaut, R. H., & Filz, G. M. (2008). Deformations and tensions in single-layer and stacked geosynthetic tubes. In *The first Pan American Geosynthetics Conference & Exhibition* (pp. 506-513). Cancun, Mexico: IFAI.

Plaut, R.H., & Suherman, S. (1998). Two-dimensional analysis of geosynthetic tubes. *Acta Mechanica*, 129(3-4), 207-218.

Ratnayesuraj, C.R., & Bhatia, S.K. (2018). Testing and analytical modeling of two-dimensional geotextile tube dewatering process. *Geosynthetics International*, 25(2), 132-149.

Satyamurthy, R., & Bhatia, S. K. (2009). Experimental evaluation of geotextile dewatering performance. In *Geosynthetics 2009* (pp. 464-473). pp. 506-513.

Wilke, M., & Cantré, S. (2016). Harbor Maintenance dredging operations-Residual characteristics after treatment by means of geosynthetic dewatering tubes. In *3rd Pan-American conference on geosynthetics, GeoAmericas* (pp. 506-513). Retrieved in October 11, 2022, from https://www.researchgate.net/publication/306916492_Harbour_maintenance_dredging_-_Residual_characteristics_after_treatment_by_means_of_geosynthetic_dewatering_tubes/link/58d12769458515520d581131/download

Wilke, M., Breytenbach, M., Reunanen, J., & Hilla, V. M. (2015). Efficient and environmentally sustainable tailings treatment and storage by geosynthetic dewatering tubes: working principles and Talvivaara case study. In *Proceedings Tailings and Mine Waste* (pp. 506-513). Retrieved in October 11, 2022, from https://open.library.ubc.ca/media/stream/pdf/59368/1.0314229/5.

Yan, S. W., & Chu, J. (2010). Construction of an offshore dike using slurry filled geotextile mats. *Geotextiles and Geomembranes*, *28*, 422-432.

Yang, Y., Wei, Z., Cao, G., Yang, Y., Wang, H., & Zhuang, S. (2019). A case study on utilizing geotextile tubes for tailings dams construction in China. *Geotextiles and Geomembranes*, *47*, 187-192.

Yee, T.W., & Lawson, C.R. (2012). Modelling the geotextile tube dewatering process. *Geosynthetics International*, 19(5), 339-353.

Yee, T.W., Lawson, C.R., Wang, Z.Y., Ding, L., & Liu, Y. (2012). Geotextile tube dewatering of contaminated sediments. Tianjin Eco-City, China. *Geotextiles and Geomembranes*, 31, 39-50.

Zhang, H., Wang, W., Liu, S., Chu, J., Sun, H., Geng, X., & Cai, Y. (2022). Consolidation of sludge dewatering in geotextile tubes under combined fill and vacuum preloading. *Journal of Geotechnical and Geoenvironmental Engineering*, *148*(6), 04022032.